Journal of Theoretical and Applied Physics
a SpringerOpen Journal

RESEARCH Open Access

Modification of surface properties of bell metal by radiofrequency plasma polymerization

Joyanti Chutia*, Arup Jyoti Choudhury, Arup Ratan Pal and Dolly Gogoi

Abstract

Radiofrequency (RF) plasma polymerization is a convenient thin film deposition process as it facilitates the synthesis of polymer films with stable physico-chemical properties suitable for various applications in microelectronic, optical, and biomedical fields. The unique properties of these plasma polymerized films as compared to the conventional ones are strongly related to the proper adjustment of the external plasma discharge parameters and selection of suitable monomer. It is also important to study the fundamental chemistry of RF plasma polymerization process, so that one can successfully correlate the internal features of the discharge with the film properties and explore their possible technological applications. The possibility of using styrene-based plasma polymer (SPP) films on bell metal as protective coatings is explored in this work. Depositions of the films are carried out in RF Ar/styrene discharge at working pressure of 1.2×10^{-1} mbar and at the RF power range of 20 to 110 W. Optical emission spectroscopy (OES) is used to study the active species generated during plasma polymerization, while Fourier transform infrared (FT-IR) and X-ray photoelectron spectroscopy (XPS) are used to analyze the internal chemical structures of the films. The protective performances of the SPP films are attempted to correlate with the results obtained from OES, FT-IR, and XPS analyses.

Keywords: Radiofrequency glow discharge, Styrene-based plasma polymer films, Optical emission spectroscopy, Water repellency, Protective coating

PACS: 52.77.-j, 52.80.Pi, 52.80.Vp, 52.77.Dq, 81.65.Kn

Background

Radiofrequency (RF) plasma polymerization is a convenient process of depositing polymer films with stable physico-chemical properties [1,2]. The features of plasma polymers include a more random structure than conventional polymers, extensive cross-linking, covalent bonding to substrates, and ease of control of thickness in the range from nanometers to micrometers [3,4]. The plasma polymer films are free from pinholes, hard, insoluble in organic solvents, and highly resistant to scratch, heat, and corrosion [5-8]. Therefore, these polymer films have also been extensively used for surface protection of metals, alloys, glasses, and plastics. Besides, these plasma polymer films are widely used as biocompatible materials, gas barrier films for food packaging, and humidity and chemical sensors [9-14].

It is well known that in RF plasma polymerization process, the physico-chemical properties of the deposited polymer films are strongly dependent on the external discharge parameters such as input RF power, gas/monomer flow rate, and working pressure [15,16]. The effect of these parameters on the properties of the deposited films can be well understood by investigating their internal chemical structures. Besides, the functionality of the plasma polymer films is mainly influenced by the nature of the monomers used [17,18]. It is also important to study the fundamental processes occurring in RF plasma polymerization, so that one can successfully correlate the internal features of the discharge with the film properties and explore their possible technological and industrial applications [19].

In this work, the results on the deposition of styrene-based plasma polymer (SPP) films from radiofrequency Ar/styrene glow discharge at working pressure of 1.2×10^{-1} mbar and in the RF power range of 20 to 110 W are reported. Styrene is preferred as starting monomer due to

* Correspondence: joyanti_c@sify.com
Institute of Advanced Study in Science and Technology, Paschim Boragaon, Garchuk, Guwahati, Assam 781035, India

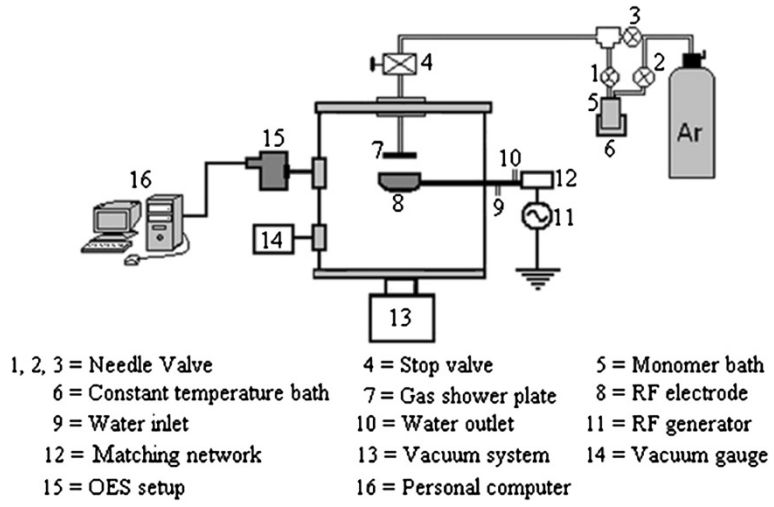

Figure 1 Schematic of the experimental setup of the RF plasma polymerization.

its high organic character and vapor pressure at room temperature [20]. The deposition of SPP films is carried out on bell metal (alloy of copper (78%) and tin (22%)) substrate which is one of the most popular types of alloys used in manufacturing items both for utilitarian (utensil, baskets, lamp, musical instrument, etc.) and esthetic (idol, ornament, picture frames, etc.) purposes [21]. However, the main disadvantage of using bell metal in such applications is that the surface of bell metal gets oxidized upon exposure to air for a short period of time. Therefore, effort has been made in this work to deposit SPP films on bell metal surface at various discharge conditions and evaluate their protective performance against severe and corrosive environment. This work also aims at studying the emission intensities of active species generated during plasma polymerization and the chemical structure of the SPP films and correlates the results with the observed properties of the films. The films are characterized by Fourier transform infrared spectroscopy (FT-IR), X-ray photoelectron spectroscopy (XPS), step profilometry, water contact angle measurement, and standard copper acetic acid salt (CASS) test (ASTM-B-368).

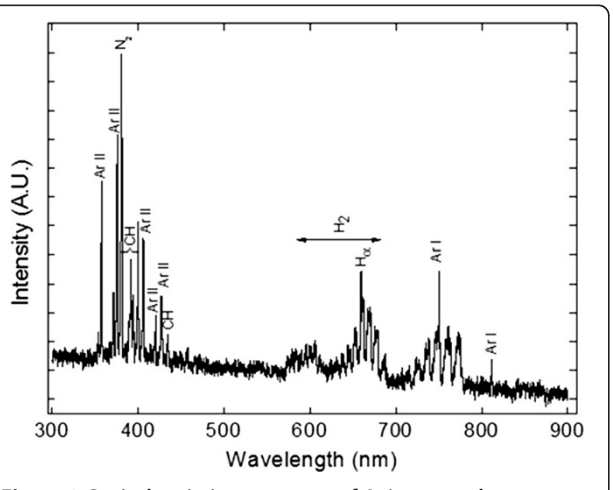

Figure 2 Optical emission spectrum of Ar/styrene plasma obtained at RF power of 80 W.

Experimental set-up

Experiments are carried out in a capacitively coupled radiofrequency (13.56 MHz) plasma device. The cylindrical vacuum chamber (Figure 1) is 40 cm in diameter and 45 cm in height. The RF electrode (10 cm in diameter) is placed at the center of the chamber and is connected to the RF generator (COMDEL-CPS-500 AS, MA, USA; 0 to 500 Watt) through an L-type matching network. During plasma polymerization, the electrode is kept cooled by circulating cold water through it. Styrene (purity > 99%, ACROS Organic, NJ, USA) is kept in a monomer bath where it is allowed to vaporize at 30°C. The argon gas is designed to flow through the monomer bath, and the gas mixture (Ar/styrene) is allowed to enter the chamber through a gas shower plate (9.25 cm in

Table 1 Species detected from the optical emission spectrum contained in Figure 2

Species	Wavelength (nm)	Transition
CH	386 to 394	$X^2\Pi$ to $B^2\Sigma^-$
Ar I	419.5	$3s^23p^5(^2P^\circ_{3/2})4s$ to $3s^23p^5(^2P^\circ_{3/2})5p$
	425.0	id[a]
	750.5	$3s^23p^5(^2P^\circ_{1/2})4s$ to $3s^23p^5(^2P^\circ_{1/2})4p$
	811.0	$3s^23p^5(^2P^\circ_{3/2})4s$ to $3s^23p^5(^2P^\circ_{3/2})4p$
CH	431.2	$A^2\Delta$ to $X^2\Pi$
H_2	583 to 670	$X^1\Sigma_g$ to $G^1\Pi_u$
H_α	656.2	$3d$ to $2p$

[a]Identical.

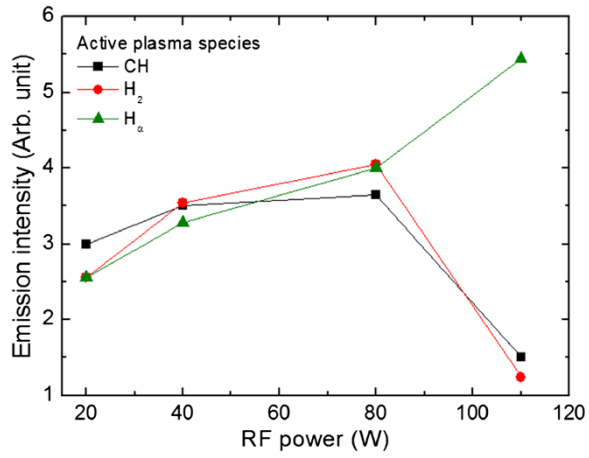

Figure 3 Variation of emission intensities of active plasma species as a function of RF power.

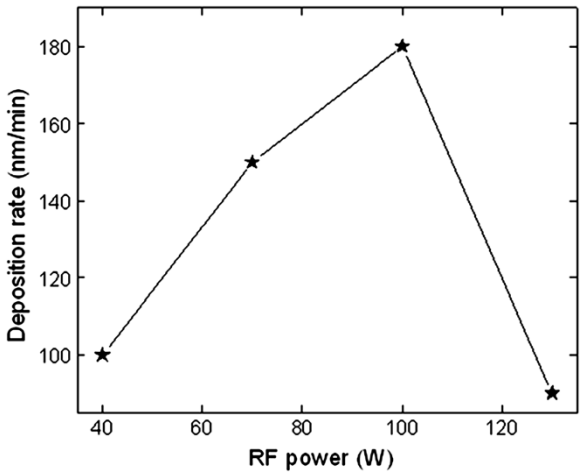

Figure 4 Variation of deposition rates of SPP films as a function of RF power.

diameter). The bottom surface of the shower plate contains 60 pierced holes, each having diameter of 5×10^{-2} cm. The flow rate of argon is controlled by a mass flow controller (Aalborg, TX, USA), whereas the flow of Ar/styrene gas mixture is controlled by precisely calibrated needle valve.

Prior to deposition, the bell metal substrates are properly cleaned using acetone, isopropyl alcohol, and distilled water. The substrates are then pretreated with argon plasma (flow rate is 5 sccm) at applied RF power of 40 W for 10 min in order to remove the native oxide present on the surfaces for enhancing film adhesion. Afterwards, the deposition process is carried out at constant working pressure of 1.2×10^{-1} mbar and RF powers ranging from 20 to 110 W. The argon flow rate is fixed at 5 sccm throughout the plasma polymerization, and the deposition time of each film is carried out for 30 min. After deposition, the RF power is kept on for 30 s so that no residue monomer gets deposited on the substrates, and the substrates are allowed to cool for 15 min in an argon flow rate of 35 sccm. The substrates are carefully taken out from the plasma chamber after 12 h and immediately transferred to a vacuum desiccator.

For optical emission spectroscopy (OES), we have used a 300-mm focal length monochromator (BENTHAM M300, Berkshire, UK) having a resolution of 0.1 nm equipped with a 1,200 lines/mm grating. The apparatus allows us to study emission lines in the range of 300 to 900 nm. A fiber optic probe is put approximately 15 cm away from the plasma source. Proper care is taken to detect maximum light emission and to avoid background radiation. The output signal is fed into a photomultiplier tube and then transferred to a personal computer through a data acquisition card. The emission spectra are recorded using LabVIEW software.

Table 2 Summary of SPP film deposition conditions

RF power (W)	Self-bias voltage (−V)	Deposition time (min)	Thickness (nm)
20	50	10	1,000
50	85		1,524
80	119		1,801
110	168		924

Film characterizations

The thickness of each SPP film is measured with a stylus step profiler (Dektak-150, Veeco Instruments, Inc., NY, USA) having vertical resolution of 1 Å (maximum).

The surface chemistry of the films is carried out by means of FT-IR and XPS. The internal chemical structures of the films are investigated by means of FT-IR (Vector 22, Bruker Corporation, MA, USA) spectroscopy

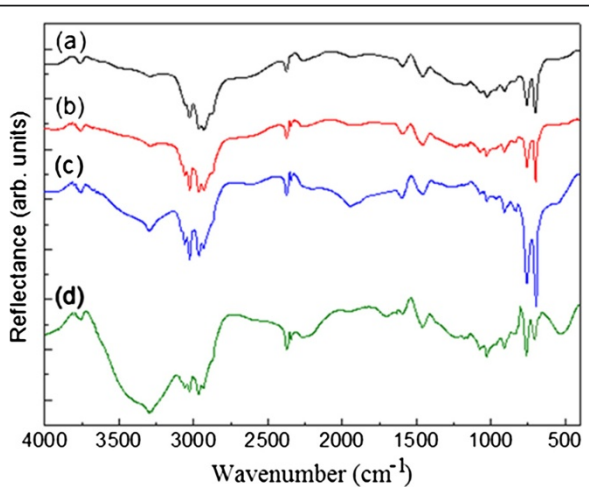

Figure 5 FT-IR spectra of the SPP films. The films are deposited at RF powers of (**a**) 20, (**b**) 50, (**c**) 80 and (**d**) 110 W.

Table 3 Assignments of peaks observed in the FT-IR spectra included in Figure 5

Wavenumber (cm^{-1})	Assignment
3,289	Hydroxyl O-H stretching
3,062 and 3,031	Aromatic C-H stretching
2,965 and 2,867	Methyl (CH_3) C-H stretching
2,928	Methylene C-H stretching
1,705	Carbonyl C = O stretching
1,595	In-plane phenyl ring bending mode
1,457	Methyl C-H bending: in-plane phenyl ring bending mode
1,361	Methyl C-H bending
1,266	In-plane C-H bending of aromatic ring
1,031	C-O stretching vibration
906	C-H out-of-plane bending
758 and 702	Out-of-plane phenyl ring bending mode

and XPS. The FT-IR spectra of the films were obtained in the transmittance mode, within the spectral range of 4,000 to 400 cm^{-1} (spectral resolution is 4 cm^{-1}), using 30° specular reflectance accessory. The XPS studies are conducted in a UHV chamber (base pressure $< 2 \times 10^{-8}$ mbar) using a VG make, CLAM-2model hemispherical analyzer with a non-monochromatic twin Al/Mg X-ray source (VG Scienta, Quebec, France). With Mg K_α line, (1,253.6 eV) detailed spectra are collected.

The hydrophobicity of the SPP films is investigated in ambient atmospheric conditions by a video-based water contact angle measurement (OCA 20, Data Physics Instruments GmbH, Filderstadt, Germany) system (experimental conditions: deionized water; 1.8 μl water drop). The system is equipped with a software-operated high-precision liquid dispenser to precisely control the drop size of the used liquid. The water droplet is dropped on the film surface through a computer-controlled process, and the image is taken immediately. The drop image is then stored via a CCD video camera using a PC-based acquisition and data processing. As the measurement of the contact angle is obtained from the image that is captured immediately, the effect of evaporation on the real measurement can be ignored. In this experiment, five point measurements on each film are randomly performed, and the average value of the five point measurements is regarded as the contact angle of the film with a standard deviation of approximately 2%. The surface energies of the SPP films are evaluated using Neumann's theory which considers only one liquid [22].

Table 4 XPS studies of the atomic compositions (%) of carbon and oxygen, and relative oxygen/carbon ratios in SPP films deposited in the RF power range of 20 to 110 W

RF power (W)	Atomic compositions (%)		
	Carbon (C)	Oxygen (O)	O/C
20	92.2	7.8	0.08
50	94.7	5.3	0.05
80	97.4	1.6	0.01
110	90.8	9.2	0.10

Atomic force microscopic (AFM) images are obtained in ambient atmospheric conditions with a digital multimode scanning probe microscope (Veeco) equipped with a nanoscope IVA controller (resolution: horizontal, 0.2 nm and vertical, 0.01 nm). The images are taken in tapping mode at a scanning rate of 1 Hz (scan size is 3×3 μm). The root-mean-square (rms) distribution profiles of the SPP films are measured by scanning probe microscopy software (WS*x*M, Nanotec Electronica S.L., Madrid, Spain).

The corrosion test on the films is carried out in a closed testing chamber (internal volume, 0.1 m^3) by standard CASS test according to ASTMB368 module

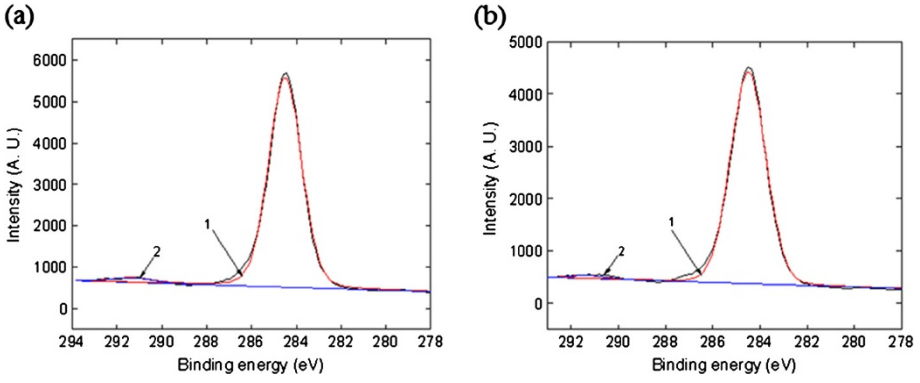

Figure 6 Curve fit of the C1 peaks of the SPP films. The films are deposited at RF powers of (**a**) 20 and (**b**) 110 W (1, C-C and/or C-H; 2, $\pi - \pi^*$ shake-up satellite).

Table 5 Curve fit of C1 peaks of the SPP films deposited in the RF power range of 20 to 110 W to study the functional units and their percentages of content in the films

Position (eV)	Assignment	Films prepared at RF power (W) of			
		20	50	80	110
285.0	C-C, C-H	96.7	97.1	98.7	95.8
291.8	$\pi - \pi^*$ shake-up satellite	3.3	2.9	1.3	4.2

(ASTM International, PA, USA). The CASS test is performed at room temperature, and the films are kept in observation for 60 h.

Results and discussion

Optical emission spectroscopy

Figure 2 shows a typical emission spectrum obtained from Ar/styrene glow discharge at working pressure of 1.2×10^{-1} mbar and RF power of 80 W. The spectra obtained at other discharge conditions (RF power 20, 50, and 110 W) reveal similar pattern as that shown in Figure 2. The main transitions that are observed in the spectrum are reported in Table 1. It is clearly seen that the spectrum contained in Figure 2 includes N_2 (380.5 nm), CH (433.2 nm), H_2 (583 to 670 nm) and H_α (656.2nm) species. The presence of N_2 in the spectrum is attributed to the residual nitrogen impurity in the deposition chamber. The H_α (656.2nm) emitted line arises from the Balmer series of atomic hydrogen, which is generally formed in glow discharge of hydrocarbon. The variation in emission intensities of the active plasma species as a function of RF power is shown in Figure 3. Species like CH, H_2, and H_α are selected for analysis as they are expected to play important role in the SPP film deposition process. It is revealed that the emission intensity of each species is strongly dependent on the variation of RF power. In the RF power range of 20 to 80 W, the relative concentration of each species (CH, H_2, and H_α) increases with power. However, at sufficiently high RF power (110 W), the emission intensities of H_2 and CH species are observed to be decreased, which can be interpreted as a result of either dissociation of H_2 and CH or their recombination with other plasma species (or both).

Film growth

The deposition conditions for SPP films at working pressure of 1.2×10^{-1} mbar and in the RF power range of 20 to 110 W are shown in Table 2. It is observed from the data presented in Table 2 that the film thickness continues to increase up to an RF power of 80 W, and then it begins to decrease with further increase in power. From the data given in Table 2, the deposition rates (nanometers per minute) of the SPP films obtained at various RF powers (20 to 110 W) are evaluated. The variation of deposition rates of SPP films as a function of RF power is shown in Figure 4. It may be seen from the plot contained in Figure 4 that highest deposition rate (180 nm/min) is observed for the SPP film deposited at RF power of 80 W. The increase in deposition rates of the films with RF power (from 40 to 100 W) may be corroborated with the results drawn from OES analyses. Also, as the RF power is increased, the plasma polymerization is transformed from low energetic state to energy sufficient state. This means that more energy per unit mass of the monomer is

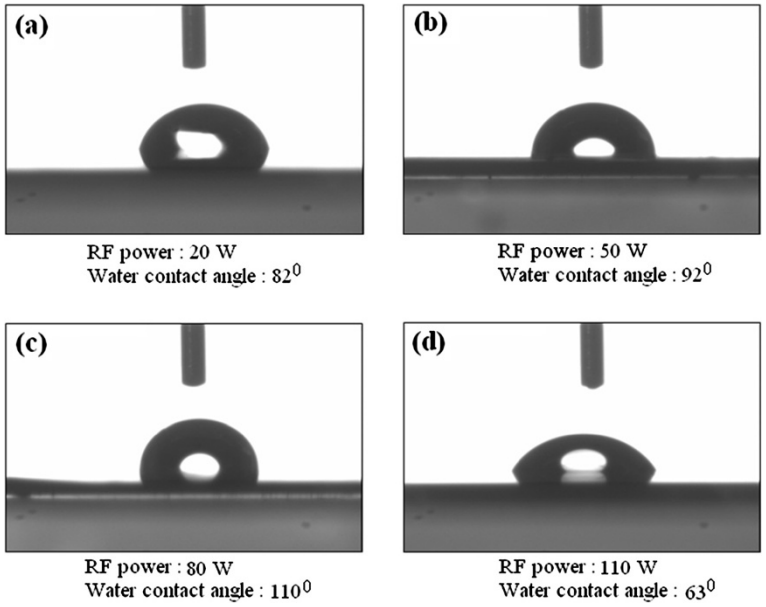

Figure 7 Variation in the shapes and contact angles of water drops on the SPP films.

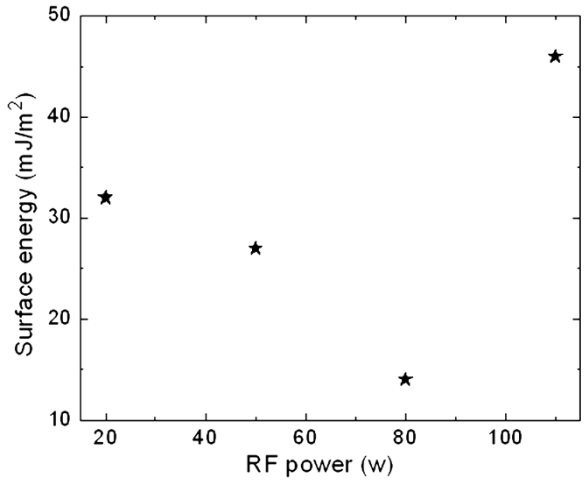

Figure 8 Variation in surface energy of the SPP films as a function of RF power.

available with increasing RF power, resulting in more fragmentation of styrene monomer, and thus leading to an increase in deposition rate of the film [23]. However, at RF power of 110 W, the deposition rate of the film is found to be decreased. This is may be due to the fact that at sufficiently high RF power, the active plasma species (ions, free radicals, etc.) acquire enough energy above a certain critical level to sputter the deposited film surface, producing a reduction in the deposition rate [24].

Fourier transform infrared spectroscopy

The FT-IR spectra of the SPP films are shown in Figure 5. The assignments of the peaks are listed in Table 3 according to the literatures [25-28]. The peak corresponding to the band at 2,965 and 2,867 cm^{-1} signifies methyl CH_3 symmetric C-H stretching vibration [25]. The presence of methyl groups is an indicator of extensive branching of SPP films. From the plots presented in Figure 5, it is observed that for SPP films deposited in the RF power range of 20 to 80 W, the absorption intensities of the peaks positioned at 702, 758 (both corresponding to out-of-plane phenyl ring bending mode), and 3031 cm^{-1} (aromatic C-H stretching mode) increase with increasing power, while for film deposited at higher RF power (110 W), the absorption intensities of the above peaks decrease [25-27]. Regarding the film

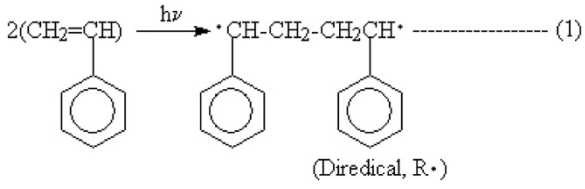

Figure 9 Initiation reaction of polystyrene to form diradical.

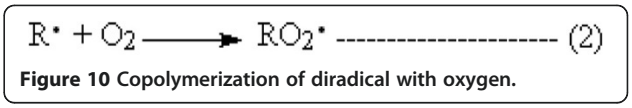

Figure 10 Copolymerization of diradical with oxygen.

deposited at RF power of 110 W, the absorption intensities of the peaks at 1,595 cm^{-1} (in-plane phenyl ring bending mode) and 2,965 cm^{-1} (methyl ($-CH_3$) C-H stretching mode) decrease compared to those deposited in the RF range of 20 to 80 W [25,28]. Moreover, it is also revealed that in comparison to films deposited in the RF power range of 20 to 80 W, a relatively strong absorption band positioned at 3,289 cm^{-1} (hydroxyl OH stretching vibration mode) appears in the spectrum of the film deposited at higher RF power (110 W) [25,28]. The band positioned at 3,289 cm^{-1} indicates reaction of trapped free radicals at the SPP films with atmospheric oxygen or water vapor. This behavior is common for plasma polymers formed by free radical mechanism [29]. From the above observations, it can be assumed that at higher RF power (110 W), the electron energy becomes sufficient enough to dissociate phenyl rings and methyl groups CH_3 present in styrene monomer. An important point to be noticed here is that no functional group containing nitrogen is detected in the FT-IR spectra. This suggests that nitrogen does not participate in the film formation process, although it shows its presence in the OES spectrum.

X-ray photoelectron spectroscopy

The atomic compositions corresponding to each SPP film deposited in the RF power range of 20 to 110 W are summarized in Table 4. The oxygen content detected in the films is assumed to be contributed by the residual oxygen present in the plasma chamber. It is seen from the data given in Table 4 that for the SPP films deposited in the RF power range of 20 to 80 W, a rise in RF power yields an increase in carbon and decrease in oxygen content in the films. On the other hand, the SPP film deposited at RF power of 110 W shows a decrease in carbon and increase in oxygen content. This indicates more dissociation of methyl groups present in styrene monomer due to dissipation of higher RF power in the plasma. To gain more insight into the chemical compositions of the

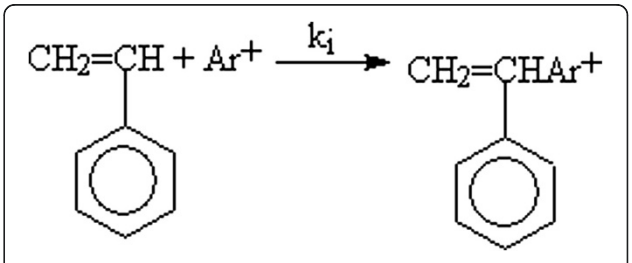

Figure 11 Formation of cationic radical during initiation.

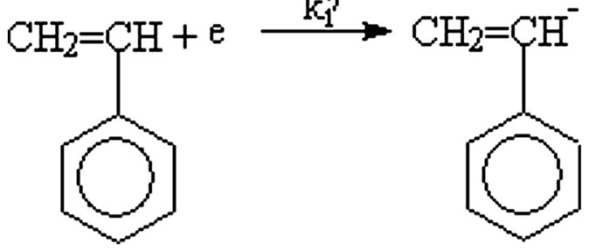

Figure 12 Formation of anionic radical during initiation.

SPP films, the curve fitting of C1 spectra for each film is performed. The fitting of C1 spectra of the SPP film deposited at RF power of 20 and 110 W is shown in Figures 6a,b. As observed from Figures 6a,b, the C1 spectra of the films has been fitted with two peaks; one large peak corresponding to C-C and/or C-H units (285 eV) and one small peak related to $\pi - \pi^*$ (291.8 eV) shake-up satellite. The characteristic $\pi - \pi^*$ shake-up satellite is due to the resonance of the aromatic rings of SPP films [30,31]. The percentages of functional units and their content in the films are given in Table 5. From the data presented Table 5, the content of C-C and/or C-H units slightly increases by 2% with the RF power (from 20 to 80 W). Moreover, plasma polymerization of styrene at RF power of 100 W results in formation of highest carbon-rich film (98.7%). In the case of film deposited at RF power of 110 W, the C-C and/or C-H units decrease to 95.8% compared to the film deposited at RF power of 80 W, and it is assumed that greater fragmentation of styrene molecules containing methyl groups ($-CH_3$) occurs at higher RF power. This assumption agrees well with the results drawn from OES and FT-IR analyses. The above discussions reveal that an increase in RF power leads to the incorporation of more organic content into the films, while at sufficiently high

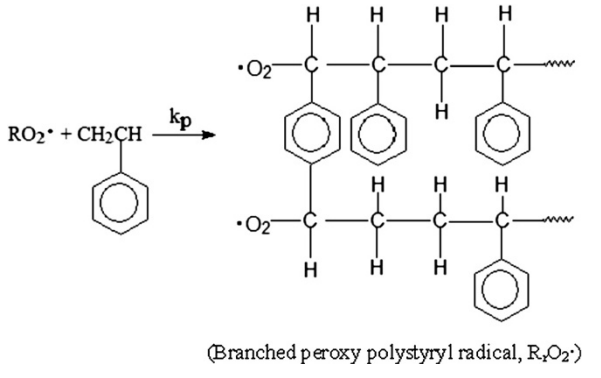

Figure 13 Propagation reaction of peroxy diradical with styrene monomer.

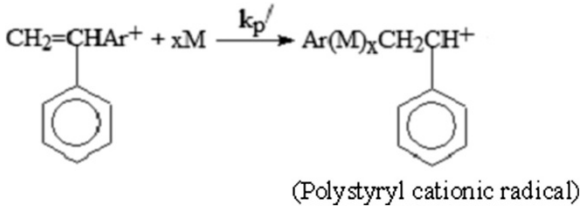

Figure 14 Propagation reaction of polystyryl cationic radical.

RF power (110 W), there is a decrease in the organic content of the films.

Water contact angle measurement

Figure 7a,b,c,d shows the variation of the shapes and contact angles of water drops on the SPP films prepared in the RF power range of 20 to 110 W. As observed from Figures 7a,b,c,d, the values of contact angle for SPP films increase from 82° to 110° when the RF power is increased from 20 to 80 W. For SPP film prepared at 110 W, the value of contact angle decreases to 63°. The variation of surface energy of the SPP films with RF power is shown in Figure 8. From Figures 7a,b,c,d and Figure 8, it is revealed that the SPP films show good hydrophobic behavior in the RF power range of 20 to 80 W, while at 110 W, the film becomes hydrophilic in nature. The variation in hydrophobic behavior of the SPP films with RF power can be explained in terms of the formation of peroxy polystyryl radical. Although the polymerization of styrene initiated by RF plasma is very complex due to occurrence of various simultaneous chemical reactions in the plasma phase, a simple mechanism may be postulated as depicted in the succeeding sections.

Initiation

Presumably the initiating species are peroxy radical and Ar+. Both the initiating steps Figure 9 and Figures 10, 11 and 12 are feasible and can occur simultaneously. At low pressure, R• copolymerizes with oxygen to form peroxy radical (Figure 10).

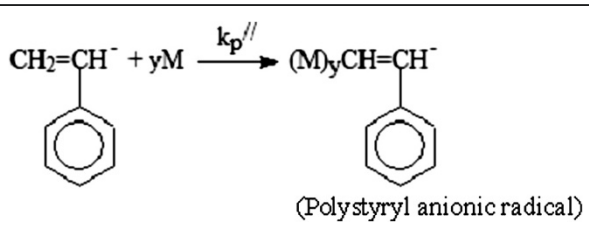

Figure 15 Propagation reaction of polystyryl anionic radical.

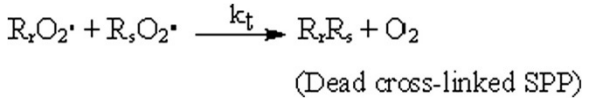

Figure 16 Termination reaction of polystyryl radical to form dead cross-linked SPP.

Propagation

There will be two types of propagations, Figure 13 and Figures 14 and 15.

Termination

The termination of polystyryl radical is also very complex. The termination may occur due to collision of the peroxy polystyryl radical on the surface of the substrate. This will lead to the formation of highly cross-linked SPP with the elimination of O_2 molecule followed by cyclization of the polystyryl radical. This step may be written as in Figure 16.

The termination process may also be due to transfer reaction of SPP, i.e., abstraction of hydrogen atom from SPP molecule by polystyryl radical (Figure 17). The termination of polystyryl radical may further occur through combination of ionic polystyryl radical leading to highly cross-linked SPP. The termination mechanism is shown in Figure 18.

It is assumed that all the above termination reactions will occur simultaneously. From XPS analyses, it is revealed that with increasing RF power (from 20 to 80 W), the peroxy polystyryl radicals progressively lose oxygen through cyclization process. It is therefore apparent that when oxygen is lost, SPP film with higher cross-linking density and improved hydrophobic character is formed. So, hydrophobic behavior of the films tends to increase when RF power is increased (from 20 to 80 W). However, at higher RF power of 110 W, the chemical structure of the SPP film surface is extensively destroyed due to high energetic ion bombardment, resulting in formation of free radicals which are trapped in the film surface. When exposed to the atmosphere, these free radicals will immediately react with the atmospheric oxygen, thereby making the film poorly hydrophobic.

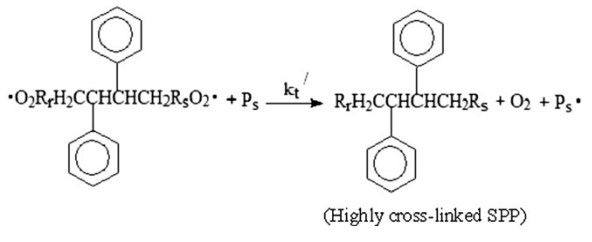

Figure 17 Termination reaction involving abstraction of hydrogen atom from SPP molecule by polystyryl radical.

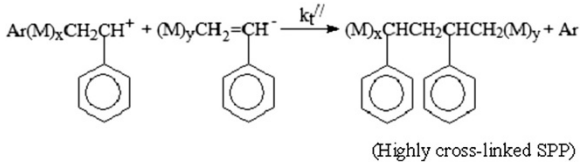

Figure 18 Termination reaction involving recombination of ionic polystyryl radicals.

Copper acetic acid salt test

Standard CASS test (ASTM-B-368) [29,30] is performed on the SPP films to study their corrosion resistance behavior. Here, a homogeneous solution is prepared from 5% sodium chloride (purity > 99%, Merck KGaA, Darmstadt, Germany) and 0.026% copper (II) chloride (purity > 99%, Merck) solution, and the pH of the solution is maintained at 3.1 by adding required amount of glacial acetic acid (purity > 99%, Merck). One-third of each film is dipped inside the solution over a total observation time of 60 h. A virgin bell metal sample dipped inside the solution serves as reference. The entire test is carried out in a dust-free environment and at room temperature. The virgin bell metal sample and the films are observed visually every 6 h. The portion of virgin bell metal surface dipped inside the solution is soon found to change its color from bright golden to blackish (at the observation time of 8 h), thereby showing corrosion of the surface. The visual image as given in Figure 19a shows the corrosion of the virgin bell metal. At the observation time of 12 h, the portion of the film deposited at RF power of 110 W (Figure 19b), dipped inside the solution, gets completely peeled off due to permeation of salt solution into its surface. Regarding film deposited at RF power of 110 W, it is further noticed from the image included in Figure 19b that the salt solution moves up into the surface resulting in more corrosion in the film. This indicates poor adhesive nature of the SPP film deposited at RF power of 110 W. Up to 12 h of observation, no sign of crack or spot is detected for the SPP films deposited at RF powers of 20, 50 and 80 W. However, at the observation time of 24 h, some parts of the film surface deposited at RF power of 20 W, kept under the salt solution is found to be peeled off. The other films show no change in their surface morphologies as observed visually. The film deposited at RF power of 20 W gets completely corroded after the observation time of 32 h. Regarding film deposited at RF power of 50 W, minute cracks are observed on its surface at an observation time of 48 h (Figure 19c). At observation time of 56 h, the cracked portion of the film deposited at RF power of 50 W is found to be stripped off, while no sign of crack/spot is observed for film deposited at RF power of 80 W (Figure 19d) even after 60 h. The results suggest that the SPP film deposited at RF power of 80 W shows relatively good corrosion resistance behavior compared to the other

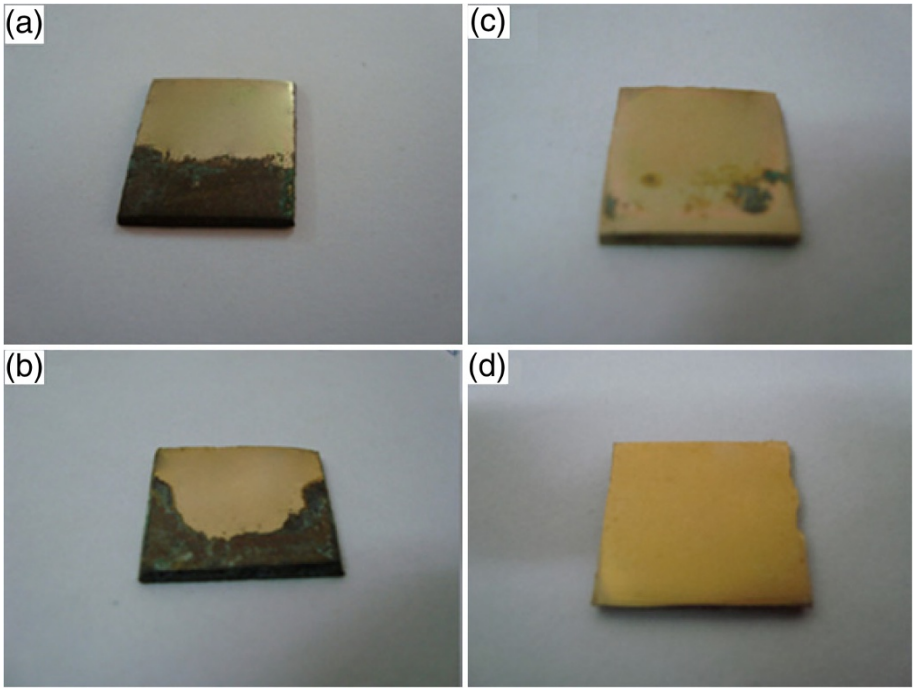

Figure 19 Images showing visually observed corrosion tested surfaces of virgin bell metal and SPP films. (**a**) Virgin bell metal and SPP films deposited at RF powers of (**b**) 110, (**c**) 50 and (**d**) 80 W.

films, which may be assumed to be contributed by the highest percentage of carbon content present in the film. Moreover, the highest emission intensity of CH species observed in the Ar/styrene plasma at 80 W is possibly another significant factor contributing to such enhanced corrosion resistance behavior of the film deposited at RF power of 80 W.

Atomic force microscopy

Figure 20a,b shows the three-dimensional AFM images of SPP films prepared at RF powers of 20 and 80 W. The AFM images of all the SPP films show quite smooth and crack-free surfaces, thereby indicating uniform deposition during Ar/styrene plasma polymerization process. The variation of rms roughness of the films with RF power is given in Table 6. The increase in rms roughness with RF power is possibly due to the sputtering of the film surface by ions, which gain more and more energy with the increase in RF power [32].

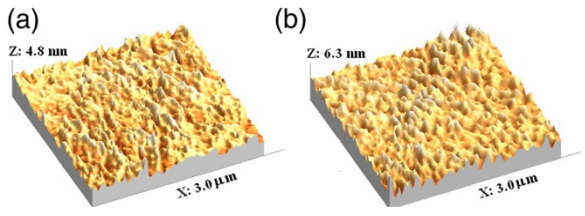

Figure 20 AFM images of SPP films. The films are deposited at RF powers of (**a**) 20 and (**b**) 80 W.

Conclusions

SPP films are successfully deposited from RF Ar/styrene glow discharge at a working pressure of 1.2×10^{-1} mbar and in the RF power range of 20 to 110 W. Maximum deposition rate (180 nm/min) is observed for the SPP film deposited at 80 W. OES, FT-IR, and XPS analyses indicate that the improved hydrophobicity and corrosion resistance behavior of the SPP film deposited at RF power of 80 W may be linked to the dominance of CH species in the glow discharge and enhanced cross-linking density due to the presence of highest percentage of carbon content in the film. Besides, more loss of oxygen by peroxy polystyryl radicals with increasing RF power (from 20 to 80 W) may also contribute to the enhancement in hydrophobic behavior of the films.

Table 6 Surface morphology parameters as determined by AFM analyses of SPP films deposited in the RF power range of 20 to 110 W

RF power (W)	rms roughness (nm)
20	0.35
50	0.48
80	0.67
110	0.87

However, at higher RF power (110 W), the SPP film becomes hydrophilic in nature and displays poor corrosion resistance behavior, which may be accounted for the extensive destruction in cross-linked chemical structure of the film by high impinging ion energy. The results suggest the possibility of using SPP film deposited at RF power of 80 W as high performance coating for surface protection of bell metal.

Competing interests
The authors declare that they have no competing interests.

Authors' contributions
The work presented here was carried out in collaboration among all authors. JC and ARP defined the research theme. AJC and DG designed the methods and experiments, carried out the laboratory experiments, analyzed the data, interpreted the results, and drafted the paper. JC and ARP discussed the analyses, interpretation, and final presentation of the paper. All authors read and approved the final manuscript.

Authors' information
JC is an Emeritus Professor at the Institute of Advanced Study in Science and Technology, Guwahati, Assam, India. JC earned her Ph.D. from Dibrugarh University, Assam, India, and her research interests includes nonlinear dynamics in plasmas, experimental plasma processing, plasma sputtering, and nano- and bio-physics. ARP is an assistant professor of the Institute of Advanced Study in Science and Technology, Guwahati, Assam, India. ARP earned his Ph.D. from Gauhati University, Assam, India, and his research interests include theoretical plasma physics, plasma polymerization for synthesis of conducting polymers, development of nanocomposite material based organic–inorganic hybrid bulk heterojunction solar cell solar cell, polymer nano-composite, fuel cell, and nano- and bio-physics. AJC is a research associate at the Institute of Advanced Study in Science and Technology, Guwahati, Assam, India, and his research field includes experimental plasma processing, material chemistry and physics and biomaterial. DG is a Ph.D. research scholar at the Institute of Advanced Study in Science and Technology, Guwahati, Assam, India.

Acknowledgements
This work was supported by a grant from the Board of Research in Nuclear Sciences, Department of Atomic Energy and the government of India. The authors would like to thank Prof. Narendra Nath Dass, IASST for the fruitful discussion regarding polymerization mechanism of styrene monomer.

Received: 30 October 2012 Accepted: 30 October 2012
Published: 28 November 2012

References
1. Lasorsa, CA, Perillo, PM, Morando, PJ: Protective $Si_xO_yC_z$ coatings on steel prepared by plasma activated chemical vapour deposition. Surf. Coat. Technol. **204**, 2813 (2010)
2. Jacob, MV, Easton, CD, Woods, GS, Berndt, CC: Fabrication of a novel organic polymer thin film. Thin Solid Films **516**, 3884 (2008)
3. Morent, R, De Geyter, N, Van Vlierberghe, S, Dubruel, P, Leys, C, Gengembre, L, Schacht, E, Paayen, E: Deposition of HMDSO-based coatings on PET substrates using an atmospheric pressure dielectric barrier discharge. Prog. Org. Coat. **64**, 304 (2009)
4. Roualdes, S, Hovnanian, N, Lee, AV, Berjoan, R, Durand, J: Organic/inorganic thin films deposited from diethoxydimethylsilane by plasma enhanced chemical vapor deposition. J. Non-Cryst. Solids **248**, 235 (1999)
5. Kuřitka, I, Horváth, P, Schauer, F, Zemek, J: Thermal stability of plasma deposited polysilanes. Polym. Degrad. Stabil. **91**, 2901 (2006)
6. Morent, R, De Geyter, N, Vlierberghe, SV, Dubruel, P, Leys, C, Schacht, E: Organic–inorganic behaviour of HMDSO films plasma-polymerized at atmospheric pressure. Surf. Coat. Technol. **203**, 1366 (2009)
7. Chapman, B: Glow Discharge Processes–Sputtering and Plasma Etching, p. 149. Wiley, New York (1980)
8. Yasuda, H: Thin Film Processes, p. 361. Academic Press, New York (1978)
9. Young-Yeon, J, Chang, HK, Hong, YC, Lee, SH: Water-repellent improvement of polyester fiber via radio frequency plasma treatment with argon/hexamethyldisiloxane (HMDSO) at atmospheric pressure. Curr. Appl. Phys. **9**, 253 (2009)
10. Gandhiraman, RP, Karkari, SK, Daniels, SM, McCraith, B: Influence of ion bombardment on the surface functionalization of plasma deposited coatings. Surf. Coat. Technol. **203**, 3521 (2009)
11. Ji, YY, Hong, YC, Lee, SH, Kim, SD, Kim, SS: Formation of super-hydrophobic and water-repellency surface with hexamethyldisiloxane (HMDSO) coating on polyethyleneteraphtalate fiber by atmosperic pressure plasma polymerization. Surf. Coat. Technol. **202**, 5663 (2008)
12. Gorblg, O, Nehlsen, S, Mtiller, J: Hydrophobic properties of plasma polymerized thin film gas selective membranes. J. Membr. Sci. **138**, 115 (1998)
13. Prasada, GR, Danielsa, S, Cameronb, DC, McNamarac, BP, Tullyd, E, O'Kennedy, R: PECVD of biocompatible coatings on 316L stainless steel. Surf. Coat. Technol. **200**, 1031 (2005)
14. Shim, J, Yoon, HG, Sang-Hyun, N, Kim, I, Kwak, S: Silicon oxynitride gas barrier coatings on poly(ether sulfone) by plasma-enhanced chemical vapor deposition. Surf. Coat. Technol. **202**, 2844 (2008)
15. Grill, A: Cold Plasma in Materials Fabrication: From Fundamental to Applications, pp. 87–97. IEEE Press, New York (1994)
16. Hegemann, D, Brunner, H, Oehr, C: Evaluation of deposition conditions to design plasma coatings like SiO_x and a-C:H on polymers. Surf. Coat. Technol. **174**, 253 (2003)
17. Borcia, G, Brown, NMD: Hydrophobic coatings on selected polymers in an atmospheric pressure dielectric barrier discharge. J. Phys. D: Appl. Phys. **40**, 1927 (2007)
18. Biederman, H, Osada, Y: Plasma Polymerization Processes, pp. 161–182. Elsevier, Amsterdam (1992)
19. Choudhury, AJ, Chutia, J, Barve, SA, Kakati, H, Pal, AR, Jagannath, Mithal, N, Kishore, R, Pandey, M, Patil, DS: Studies of physical and chemical properties of styrene-based plasma polymer films deposited by radiofrequency Ar/styrene glow discharge. Prog. Org. Coat. **70**, 75 (2011)
20. Network Solutions: Ineos-Nova: http://www.ineos-nova.com/Products/ChemicalsCM/documents/Styrene_Monomer_Safety_Guide.pdf. Accessed 30 January 2012
21. Das, M, Bayan, B, Choudhury, B: Socio-economic aspects of bell metal industry workers of Sarukhetri Block of Barpeta District. Assam. Econ. Aff. **56**, 147 (2011)
22. Kwok, DY, Lam, CNC, Li, A, Leung, A, Wu, R, Mok, E, Neumann, AW: Measuring and interpreting contact angles: a complex issue. Colloids Surf. A **142**, 219 (1998)
23. Timothy, T, Yuen, Y, Leong, H, Yong, T, Zhou, Y: Coating of polystyrene thin film on glass for protein immobilization in optical biosensor applications. Lieberman, RA, Asundi, AK, Asanuma, H (eds.) Advanced photonic sensors and applications. Proceedings of SPIE, vol 3897, p. 150. SPIE, Washington (1999)
24. Geckeler, KE, Gebhardt, R, Grunwald, H: Surface modification of polyethylene by plasma grafting with styrene for enhanced biocompatibility. Naturwissenschaften **84**, 150 (1997)
25. Shen, DY: Application of Infrared Analysis Methods in Polymers, p. 69. Scientific, Beijing (1983)
26. Dyer, JR: Applications of Absorption Spectroscopy of Organic Compounds, pp. 22–32. Prentice-Hall, New Jersey (1978)
27. Jesch, K, Bloor, JE, Kronick, P: Structure and physical properties of glow discharge polymers. I. Polymers from hydrocarbons. J. Polym. Sci **Part A 4**, 1487 (1966)
28. Pavia, DL, Lampman, GM, Kriz, GS: Introduction to Spectroscopy, pp. 27–72. Harcourt College, Orlando (1996)
29. Ozden, B, Hacaloglu, J, Akovali, G: A mass spectrometric study on plasma reactions of styrene and methyl methacrylate. Eur. Polym. J. **27**, 1405 (1991)
30. Wang, MJ, Chang, YI, Epaillard, FP: Acid and basic functionalities of nitrogen and carbon dioxide plasma-treated polystyrene. Surf. Interf. Anal. **37**, 348–355 (2005)
31. Nakao, A, Suzuki, Y, Iwaki, M: Water wettability and zeta-potential of polystyrene surface modified by Ne or Na implantation. J. Colloid Interf. Sci. **197**, 257 (1998)
32. Sahil, S, Segui, Y, Ramdani, R, Takkouk, Z: R.f. plasma deposition from hexamethyldisiloxane-oxygen mixtures. Thin Solid Films **250**, 206 (1994)

doi:10.1186/2251-7235-6-40
Cite this article as: Chutia *et al.*: **Modification of surface properties of bell metal by radiofrequency plasma polymerization.** *Journal of Theoretical and Applied Physics* 2012 **6**:40.